Loop currents in ladder cuprates: A dynamical mean field theory study

Xiancong Lu[1] and D. Sénéchal[2]
[1]*Department of Physics, Xiamen University, Xiamen 361005, China*
[2]*Département de physique and Institut quantique, Université de Sherbrooke, Sherbrooke, Québec, Canada J1K 2R1*

(Received 10 June 2020; accepted 3 August 2020; published 18 August 2020)

We investigate the possibility of spontaneous loop currents in the two-leg ladder cuprate $Sr_{14-x}Ca_xCu_{24}O_{41}$ by applying cluster dynamical mean field theory (CDMFT) to a seven-band Hubbard model for that compound, with an exact diagonalization solver. We sample several values of the local interaction U_d and of the Cu-O energy difference E_{pd}, by applying an external field that induces loop currents. We find no instance of spontaneous loop currents once the external field is brought to zero.

DOI: 10.1103/PhysRevB.102.085135

I. INTRODUCTION

One of the most interesting features of cuprate superconductors is the pseudogap phenomenon, which is widely believed to be a key to understanding the mechanism of high-temperature superconductivity (HTSC) [1]. However, the origin of the pseudogap is still a matter of debate and the possibility of a spontaneously broken symmetry at low temperature within that state has not been excluded [2]. One important possibility is the loop currents (LC) phase, proposed by Varma [3–5], in which equilibrium orbital currents are circulating along the O-Cu-O plaquette within each unit cell, thus breaking time-reversal symmetry while preserving translational symmetry. Varma's proposal has stimulated many experimental searches for the signature of microscopic orbital magnetic moments. Polarized neutron diffraction (PND) experiments have lent support to the existence of an intra-unit-cell (IUC) magnetic order on CuO_2 planes [6–8] or involving apical oxygens [9]. By contrast, nuclear magnetic resonance (NMR) [10–12] and muon spin rotation (μSR) [13–16] have not found evidence of magnetic order. Varma's hypothesis has also been investigated theoretically, with numerical methods and models often used in the study of strongly correlated electrons, such as exact diagonalizations (ED) [17–19], variational Monte Carlo (VMC) [20,21], and the variational cluster approximation (VCA) [22]. For the three-band Hubbard model with realistic parameters for high-T_c cuprates, the results of these different methods are consistent: the LC phase is not stabilized as a ground state in the thermodynamic limit.

The existence of LCs was also investigated theoretically in the two-leg ladder, which is simpler and interpolates between one- and two-dimensional systems. By using the highly accurate density-matrix renormalization group (DMRG) technique, evidence for the existence of a "staggered-flux" phase was found for the two-leg ladder with long-range interaction both at and away from half-filling [23,24]. Analytical studies using a bosonization/renormalization group (RG) method also found stable regions of LCs for weak interactions [25,26]. However, a DMRG study on two-leg CuO ladders has found negative evidence towards the LC phase [27,28].

Recently, using polarized neutron diffraction, Bounoua *et al.* [29] discovered the existence of a new kind of short-range magnetism in the two-leg ladder cuprate $Sr_{14-x}Ca_xCu_{24}O_{41}$(SCCO-$x$) for two Ca contents ($x = 5$ and 8). The measured magnetic structure factor can be reproduced by assuming a set of counter-propagating LCs around each Cu atom. This raises the possibility of a LC phase in the ladder cuprate. In this paper, we try to verify this for $x = 8$ using cluster dynamical mean field theory (CDMFT) applied on a multiband Hubbard model.

II. MODEL AND METHOD

A. Hamiltonian

The structure of SCCO-x consists of an alternating stack of 1D CuO_2 chains and quasi-1D Cu_2O_3 two-leg ladder layers. We will focus of the ladder layer only and use a simplified description in terms of seven orbitals per unit cell: two Cu $d_{x^2-y^2}$ orbitals (in blue in Fig. 1), two O p_x and three O p_y orbitals, respectively, in green and red on the right panel of Fig. 1. The hopping amplitudes will be chosen to be the same as the ones often used in the three-band model for the cuprates, except that two of the oxygen sites in the unit cell involve both p_x and p_y orbitals, owing to the slightly different geometry of the model compared to the cuprates. The noninteracting Hamiltonian has the form

$$H_0 = \sum_{\mathbf{k},\sigma} \mathbf{t}_\mathbf{k} C^\dagger_{\mathbf{k},\sigma} C_{\mathbf{k},\sigma}, \tag{1}$$

where $C_{\mathbf{k},\sigma}$ stands for an array of annihilation operators associated with the seven orbitals per unit cell, as labeled on Fig. 1, and where the momentum-dependent matrix $\mathbf{t}_\mathbf{k}$ is shown in Eq. (2) below. That matrix is Hermitian (the upper triangle is not shown). The hopping amplitude between Cu and O orbitals is t_{pd} and the energy difference between O

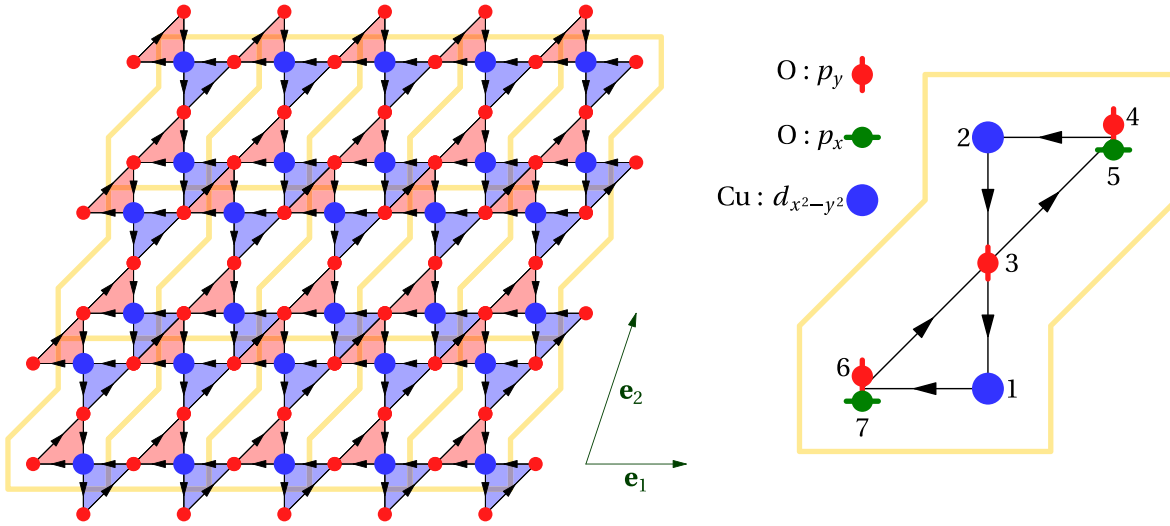

FIG. 1. (Left) Cu_2O_3 lattice. Cu atoms are in blue, oxygen atoms in red. The expected loop currents for SCCO-8 are shown by arrows and the associated fluxes of opposite signs are indicated by blue and red triangles. Unit cells are delimited in yellow and the lattice vectors $\mathbf{e}_1$ and $\mathbf{e}_2$ are shown. (Right) Seven orbitals in a given unit cell, with their labels as they appear in Eq. (2).

and Cu orbitals is E_{pd}. We assume for simplicity that the diagonal hopping amplitude t_{pp} between oxygens is the same for $p_x - p_x$ and $p_x - p_y$ bonds. We will set $t_{pp} = 1$ and $t_{pd} = 1.5$ throughout (t_{pp} sets the energy scale). Finally, we will specifically investigate the loop current structure illustrated on Fig. 1 which, according to Ref. [29], is appropriate for $x = 8$, corresponding to a doping of ∼17%. We will, however, cover a fairly wide doping range around that value.

$$\mathbf{t}_{\mathbf{k}} = -\begin{pmatrix} 0 & & & & & & \\ 0 & 0 & & & & & \\ -t_{pd} & t_{pd} & -E_{pd} & & & & \\ t_{pd}e^{-i\mathbf{k}\cdot\mathbf{e}_2} & 0 & t_{pp}(1+e^{-i\mathbf{k}\cdot\mathbf{e}_1}) & -E_{pd} & & & \\ 0 & t_{pd}(-1+e^{-i\mathbf{k}\cdot\mathbf{e}_1}) & t_{pp}(1-e^{-i\mathbf{k}\cdot\mathbf{e}_1}) & 0 & -E_{pd} & & \\ 0 & -t_{pd}e^{i\mathbf{k}\cdot\mathbf{e}_2} & 0 & t_{pp}(1+e^{i\mathbf{k}\cdot\mathbf{e}_1})e^{i\mathbf{k}\cdot\mathbf{e}_2} & t_{pp}(1-e^{i\mathbf{k}\cdot\mathbf{e}_1})e^{i\mathbf{k}\cdot\mathbf{e}_2} & -E_{pd} & \\ t_{pd}(1-e^{i\mathbf{k}\cdot\mathbf{e}_1}) & 0 & t_{pp}(1-e^{i\mathbf{k}\cdot\mathbf{e}_1}) & t_{pp}(1-e^{i\mathbf{k}\cdot\mathbf{e}_1})e^{i\mathbf{k}\cdot\mathbf{e}_2} & 0 & t_{pp}(1+e^{i\mathbf{k}\cdot\mathbf{e}_1})e^{i\mathbf{k}\cdot\mathbf{e}_2} & -E_{pd} \end{pmatrix}. \quad (2)$$

To this noninteracting Hamiltonian we add Hubbard and extended interactions on the Cu and O atoms, so that the complete Hamiltonian reads

$$H = H_0 + U_d \sum_{i\in\mathrm{Cu}} n^d_{i\uparrow} n^d_{i\downarrow} + U_p \sum_{j\in\mathrm{O}} n^p_{j\uparrow} n^p_{j\downarrow} + V_{pd} \sum_{\langle i,j\rangle, i\in\mathrm{Cu}} n^d_i n^p_j - \mu \hat{N}_{\mathrm{tot}}, \quad (3)$$

where the sum over i runs over Cu sites, the sum over j runs over the five O orbitals in each unit cell, $\langle i, j\rangle$ stands for nearest-neighbor sites (O-Cu), μ is the chemical potential, and $\hat{N}_{\mathrm{tot}}$ the total number of electrons in all the orbitals considered. U_d and U_p are the Coulomb repulsion of two holes sitting on the same copper orbital or the same oxygen orbital, respectively. V_{pd} is the Coulomb interaction between nearest-neighbor Cu and O orbitals.

B. Impurity model

In order to reveal loop currents possibly arising in model (3), we use cluster dynamical mean-field theory (CDMFT) [30–33] with an exact diagonalization solver at zero temperature (or ED-CDMFT). In CDMFT, the infinite lattice is tiled into identical units, or clusters, each of which is then coupled to a bath of uncorrelated, auxiliary orbitals. The parameters describing this bath (energy levels, hybridization, etc.) are then found by imposing a self-consistency condition.

In this work, the cluster consists of a single unit cell (as shown on the right panel of Fig. 1), which is coupled to a bath of four uncorrelated orbitals. The Cu orbitals being the most correlated (because U_d is considerably larger than U_p), we choose a simplified bath parametrization in which the bath orbitals are hybridized with the Cu orbitals only, even though $U_p \neq 0$, as shown on Fig. 2. The corresponding *Anderson impurity model* (AIM) Hamiltonian is

$$H_{\mathrm{imp}} = H_c + \sum_{i,r} \theta_{ir}(c^\dagger_i a_r + \mathrm{H.c.}) + \sum_r \epsilon_r a^\dagger_r a_r, \quad (4)$$

where H_c is the Hamiltonian (3), but restricted to a single cluster; cluster orbitals are labeled by the index i and uncorrelated (bath) orbitals by the index r. θ_{ir} is a complex hybridization parameter between cluster orbital i and bath orbital r, and ϵ_r is the energy level of bath orbital r. All these parameters are

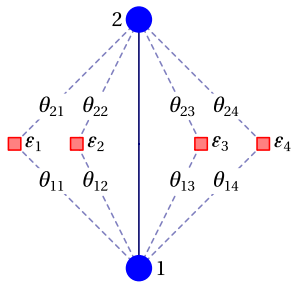

FIG. 2. Structure of the hybridization between the four bath orbitals of the Anderson impurity model and the two Cu orbitals of the cluster (for simplicity, the oxygen orbitals are not shown, even though they are part of the impurity model).

assumed to be spin independent, as we are not looking for magnetic ordering.

In ED-CDMFT, the bath parameters θ_{ir} and ϵ_r are determined by an approximate self-consistent procedure, as proposed initially in Ref. [34], that goes as follows: (i) initial values $\{\epsilon_r, \theta_{ir}\}$ are chosen on the first iteration. (ii) For each iteration, the AIM (4) is solved, i.e., the cluster Green function $\mathbf{G}_c(\omega)$ is computed using the Lanczos method. The latter can be expressed as

$$\mathbf{G}_c(\omega)^{-1} = \omega - \mathbf{t}_c - \mathbf{\Gamma}(\omega) - \mathbf{\Sigma}_c(\omega), \tag{5}$$

where $\mathbf{t}_c$ is the one-body matrix in the cluster part of the impurity Hamiltonian $H_{\rm imp}$, $\mathbf{\Sigma}_c(\omega)$ is the associated self-energy and $\mathbf{\Gamma}(\omega)$ is the bath hybridization matrix:

$$\Gamma_{ij}(\omega) = \sum_r \frac{\theta_{ir}\theta^*_{jr}}{\omega - \epsilon_r}. \tag{6}$$

(iii) The bath parameters are updated, by minimizing the distance function:

$$d(\boldsymbol{\epsilon}, \boldsymbol{\theta}) = \sum_{i\omega_n} W(i\omega_n)[\mathbf{G}_c(i\omega_n)^{-1} - \bar{\mathbf{G}}(i\omega_n)^{-1}], \tag{7}$$

where $\bar{\mathbf{G}}(\omega)$, the projected Green function, is defined as

$$\bar{\mathbf{G}}(\omega) = \frac{1}{N}\sum_{\mathbf{k}} \mathbf{G}(\mathbf{k}, \omega), \quad \mathbf{G}(\mathbf{k}, \omega) = \frac{1}{\omega - \mathbf{t}_\mathbf{k} - \mathbf{\Sigma}_c(\omega)}. \tag{8}$$

In the above, $\mathbf{t}_\mathbf{k}$ is the one-body Hamiltonian (2) and N is the (nearly infinite) number of sites. The matrices in the above are 7×7, for each spin projection. Essentially, $\bar{\mathbf{G}}(\omega)$ is the local Green function obtained by carrying the self-energy $\mathbf{\Sigma}_c(\omega)$ to the whole lattice. Ideally, $\bar{\mathbf{G}}(\omega)$ should coincide with the impurity Green function $\mathbf{G}_c(\omega)$, but the finite number of bath parameters does not allow for this correspondence at all frequencies, and so a distance function $d(\epsilon_r, \theta_{ir})$ is defined, with emphasis on low frequencies along the imaginary axis. The weight function $W(i\omega_n)$ is where the method has some arbitrariness; in this work $W(i\omega_n)$ is taken to be a constant for all Matsubara frequencies lower than a cutoff $\omega_c = 2t_{pp}$, with a fictitious temperature $\beta^{-1} = t_{pp}/50$. (iv) We go back to step (ii) and iterate until the bath parameters or the bath hybridization function $\mathbf{\Gamma}(\omega)$ stop varying within some preset tolerance.

A comment on the extended interaction H_V [the V_{pd} term in Eq. (3)]. It is split into two: $H_V = H_V^{(c)} + H_V^{(ic)}$. The first term contains the Cu-O bonds located within the clusters and is included in the impurity Hamiltonian. The second term contains the bonds located across clusters and is treated in the Hartree approximation, as explained in Ref. [35]. The self-consistent Hartree procedure is carried out at the same time as the DMFT iterations and typically converges faster than the bath parameters themselves.

III. RESULTS AND DISCUSSION

In order to probe the possible existence of loop currents in model (3), we first need to define an operator representing them. We selected the following current loop operator, defined within the unit cell and following the arrows shown on the right panel of Fig. 1:

$$\hat{I} = i(c_1^\dagger c_7 + c_7^\dagger c_3 + c_3^\dagger c_5 + c_5^\dagger c_2 + c_2^\dagger c_3 + c_3^\dagger c_1) + \text{H.c.} \tag{9}$$

We then impose an external field I proportional to this operator on the system, i.e., we replace Hamiltonian (3) by $H + I\hat{I}$. This external field induces a nonzero expectation value $\langle\hat{I}\rangle$ on the impurity model. We then reduce this external field to zero through a sequence of values (see Fig. 3) and monitor the expectation value $\langle\hat{I}\rangle$. If spontaneous currents were possible, a nonzero value of $\langle\hat{I}\rangle$ would persist down to $I = 0$, which would indicate a spontaneous breaking of time reversal symmetry (TRS). This is impossible if the hybridization θ_{ir} is purely real. One can always require the hybridization parameter θ_{1r} to be real, because of an arbitrariness in the phase of the bath annihilation operator $a_{r\sigma}$. This being done, the phase of the other hybridization θ_{2r} is determined by the CDMFT procedure. The complex-valued character of θ_{2r} is a necessary (but not sufficient) condition for a broken TRS state.

We have carried out a series of CDMFT computations on model (3) with band parameters $t_{pp} = 1$ and $t_{pd} = 1.5$, $U_p = 3$, $V_{pd} = 1$, and several values of E_{pd} (0, 2, 4, 7), U_d (6, 8, 10, 14), and chemical potential. In all cases, an external current field I was applied sequentially ($I = 0.2$, 0.1, 0.05, 0.01 and 0.0) in order to maximize the chances of finding a spontaneous current. In all cases, no such current was found: $\langle\hat{I}\rangle = 0$, within numerical error (10^{-6}). Plots of $\langle\hat{I}\rangle$ versus the electron density n_c on the impurity (corresponding to a few values of the chemical potential μ) are shown on Fig. 3. In each panel, the different curves correspond to different values of the external current field I, down to $I = 0$ for the null curve. A few sample values of U_d and E_{pd} were chosen for the figure. Another series of computations was carried out with $V_{pd} = 0$ (not shown), with the same conclusions.

In Fig. 1, another current loop may be defined, that straddles four different unit cells, meeting at its center (dotted line on the figure). An operator $\hat{I}'$ exists for this current loop, except that it is defined on the lattice model only, not on the impurity. Nevertheless, it is possible to formally compute the average of such an operator, from the lattice Green function $\mathbf{G}(\mathbf{k}, \omega)$ of Eq. (8). We have checked that this average too is identically zero in the limit of zero external field.

We have also checked that our conclusions are unchanged if we add a sizable second-neighbor O-O hopping term $t'_{pp} = -1$. This hopping was deemed important to detect loop

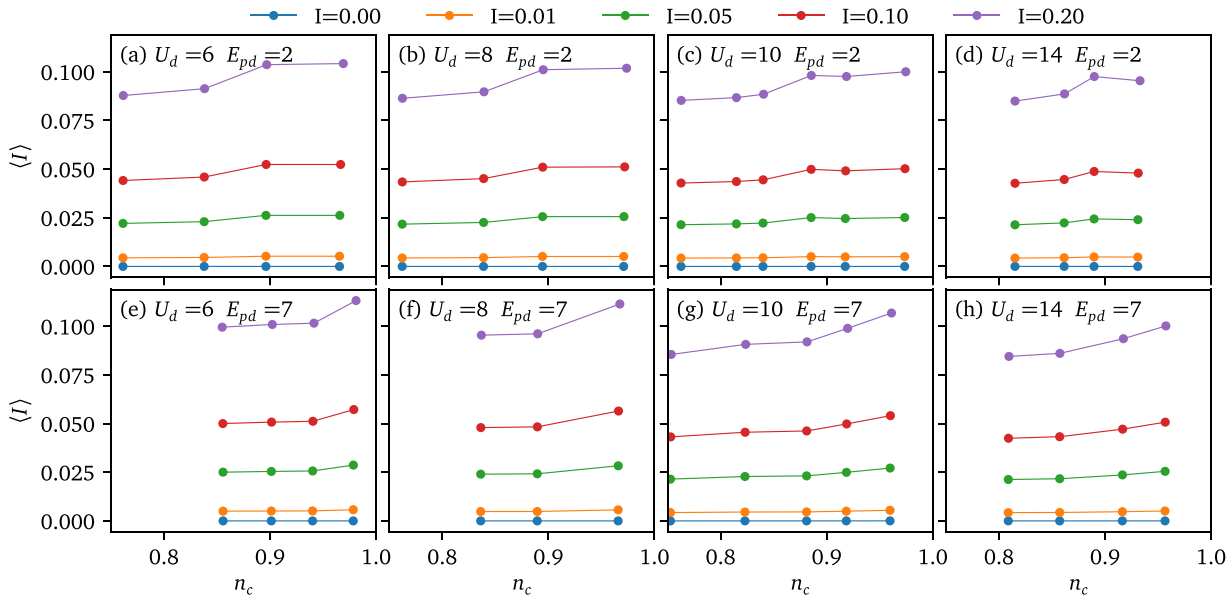

FIG. 3. Expectation value $\langle \hat{I} \rangle$ of the local current operator as a function of electron density for several values of the external field I, for several values of U_d and E_{pd}. In all cases, $t_{pd} = 1.5$, $t_{pp} = 1$, $U_p = 3$, and $V_{pd} = 1$. In the absence of external field ($I = 0$), the loop current $\langle \hat{I} \rangle$ always vanishes.

currents in Ref. [21]. In our work, such a coupling does not affect the impurity model, but affects the CDMFT solution through the self-consistency solution.

Even though we are bound to limit ourselves to a sampling of model parameters, we are strongly inclined to conclude that spontaneous orbital currents do not occur in the model we used to describe $Sr_{14-x}Ca_xCu_{24}O_{41}$. If the results of Ref. [29] are truly the signature of loop currents, the source of the discrepancy has to be found either in the model itself, or in the simple CDMFT treatment we have put in place. We have chosen an impurity model that contains a pair of triangular loops within the cluster, so as not to rely only on the measurement of lattice-based operators (as opposed to impurity-based operators). Of course the bath system itself is limited in size, but this is necessary in order to keep the problem numerically manageable. Increasing the number of bath orbitals would in general lead to better accuracy, but would not, from experience, change the nature of the ground state. Quantum Monte Carlo studies are impossible here, because of the sign problem, which becomes a phase problem for complex-valued Hamiltonians. In short, we do not believe that incremental improvements in the DMFT treatment of this problem would lead to different conclusions.

ACKNOWLEDGMENTS

We thank A.-M. Tremblay for discussions and comments. Computing resources were provided by Compute Canada and Calcul Québec. X.L. is supported by the National Natural Science Foundation of China (Grant No. 11974293) and the Fundamental Research Funds for Central Universities (Grant No. 20720180015).

[1] T. Timusk and B. Statt, Rep. Prog. Phys. **62**, 61 (1999).
[2] B. Keimer, S. A. Kivelson, M. R. Norman, S. Uchida, and J. Zaanen, Nature (London) **518**, 179 (2015).
[3] C. M. Varma, Phys. Rev. Lett. **83**, 3538 (1999).
[4] C. M. Varma, Phys. Rev. B **73**, 155113 (2006).
[5] A. Shekhter and C. M. Varma, Phys. Rev. B **80**, 214501 (2009).
[6] B. Fauqué, Y. Sidis, V. Hinkov, S. Pailhès, C. T. Lin, X. Chaud, and P. Bourges, Phys. Rev. Lett. **96**, 197001 (2006).
[7] H. A. Mook, Y. Sidis, B. Fauqué, V. Balédent, and P. Bourges, Phys. Rev. B **78**, 020506(R) (2008).
[8] L. Mangin-Thro, Y. Li, Y. Sidis, and P. Bourges, Phys. Rev. Lett. **118**, 097003 (2017).
[9] Y. Li, V. Balédent, N. Barišić, Y. Cho, B. Fauqué, Y. Sidis, G. Yu, X. Zhao, P. Bourges, and M. Greven, Nature (London) **455**, 372 (2008).
[10] S. Strässle, B. Graneli, M. Mali, J. Roos, and H. Keller, Phys. Rev. Lett. **106**, 097003 (2011).
[11] A. M. Mounce, S. Oh, J. A. Lee, W. P. Halperin, A. P. Reyes, P. L. Kuhns, M. K. Chan, C. Dorow, L. Ji, D. Xia, X. Zhao, and M. Greven, Phys. Rev. Lett. **111**, 187003 (2013).
[12] T. Wu, H. Mayaffre, S. Krämer, M. Horvatić, C. Berthier, W. N. Hardy, R. Liang, D. A. Bonn, and M.-H. Julien, Nat. Commun. **6**, 6438 (2015).
[13] G. J. MacDougall, A. A. Aczel, J. P. Carlo, T. Ito, J. Rodriguez, P. L. Russo, Y. J. Uemura, S. Wakimoto, and G. M. Luke, Phys. Rev. Lett. **101**, 017001 (2008).
[14] J. E. Sonier, V. Pacradouni, S. A. Sabok-Sayr, W. N. Hardy, D. A. Bonn, R. Liang, and H. A. Mook, Phys. Rev. Lett. **103**, 167002 (2009).
[15] W. Huang, V. Pacradouni, M. P. Kennett, S. Komiya, and J. E. Sonier, Phys. Rev. B **85**, 104527 (2012).

[16] A. Pal, K. Akintola, M. Potma, M. Ishikado, H. Eisaki, W. N. Hardy, D. A. Bonn, R. Liang, and J. E. Sonier, Phys. Rev. B **94**, 134514 (2016).
[17] M. Greiter and R. Thomale, Phys. Rev. Lett. **99**, 027005 (2007).
[18] R. Thomale and M. Greiter, Phys. Rev. B **77**, 094511 (2008).
[19] Y. F. Kung, C.-C. Chen, B. Moritz, S. Johnston, R. Thomale, and T. P. Devereaux, Phys. Rev. B **90**, 224507 (2014).
[20] C. Weber, A. Läuchli, F. Mila, and T. Giamarchi, Phys. Rev. Lett. **102**, 017005 (2009).
[21] C. Weber, T. Giamarchi, and C. M. Varma, Phys. Rev. Lett. **112**, 117001 (2014).
[22] X. Lu, L. Chioncel, and E. Arrigoni, Phys. Rev. B **85**, 125117 (2012).
[23] J. B. Marston, J. O. Fjærestad, and A. Sudbø, Phys. Rev. Lett. **89**, 056404 (2002).
[24] U. Schollwöck, S. Chakravarty, J. O. Fjærestad, J. B. Marston, and M. Troyer, Phys. Rev. Lett. **90**, 186401 (2003).
[25] E. Orignac and T. Giamarchi, Phys. Rev. B **56**, 7167 (1997).
[26] P. Chudzinski, M. Gabay, and T. Giamarchi, Phys. Rev. B **78**, 075124 (2008).
[27] S. Nishimoto, E. Jeckelmann, and D. J. Scalapino, Phys. Rev. B **79**, 205115 (2009).
[28] S. Nishimoto, E. Jeckelmann, and D. Scalapino, Physica C **470**, S53 (2010).
[29] D. Bounoua, L. Mangin-Thro, J. Jeong, R. Saint-Martin, L. Pinsard-Gaudart, Y. Sidis, and P. Bourges, Commun. Phys. **3**, 123 (2020).
[30] A. I. Lichtenstein and M. I. Katsnelson, Phys. Rev. B **62**, R9283 (2000).
[31] G. Kotliar, S. Y. Savrasov, G. Pálsson, and G. Biroli, Phys. Rev. Lett. **87**, 186401 (2001).
[32] A. Liebsch, H. Ishida, and J. Merino, Phys. Rev. B **78**, 165123 (2008).
[33] D. Sénéchal, in *Many-Body Physics: From Kondo to Hubbard*, edited by E. Pavarini, E. Koch, and P. Coleman (Forschungszentrum Jülich, Jülich, Germany, 2015), Vol. 5, pp. 13.1–13.22.
[34] M. Caffarel and W. Krauth, Phys. Rev. Lett. **72**, 1545 (1994).
[35] J. P. L. Faye, P. Sahebsara, and D. Sénéchal, Phys. Rev. B **92**, 085121 (2015).